

2015

Correlation of CsK₂Sb Photocathode Lifetime With Antimony Thickness

M. A. Mamun
Old Dominion University

C. Hernandez-Garcia

M. Poelker

A. A. Elmustafa
Old Dominion University, aelmusta@odu.edu

Follow this and additional works at: https://digitalcommons.odu.edu/mae_fac_pubs

 Part of the [Aerospace Engineering Commons](#), and the [Mechanical Engineering Commons](#)

Repository Citation

Mamun, M. A.; Hernandez-Garcia, C.; Poelker, M.; and Elmustafa, A. A., "Correlation of CsK₂Sb Photocathode Lifetime With Antimony Thickness" (2015). *Mechanical & Aerospace Engineering Faculty Publications*. 7.
https://digitalcommons.odu.edu/mae_fac_pubs/7

Original Publication Citation

Mamun, M. A., Hernandez-Garcia, C., Poelker, M., & Elmustafa, A. A. (2015). Correlation of CsK₂Sb photocathode lifetime with antimony thickness. *APL Materials*, 3(6), 1-7. doi: 10.1063/1.4922319

Correlation of CsK₂Sb photocathode lifetime with antimony thickness

M. A. Mamun,^{1,2,a} C. Hernandez-Garcia,³ M. Poelker,³ and A. A. Elmustafa^{1,2}

¹Department of Mechanical and Aerospace Engineering, Old Dominion University, Norfolk, Virginia 23529, USA

²The Applied Research Center, Thomas Jefferson National Accelerator Facility, Newport News, Virginia 23606, USA

³Thomas Jefferson National Accelerator Facility, Newport News, Virginia 23606, USA

(Received 12 April 2015; accepted 27 May 2015; published online 10 June 2015)

CsK₂Sb photocathodes with quantum efficiency on the order of 10% at 532 nm, and lifetime greater than 90 days at low voltage, were successfully manufactured via co-deposition of alkali species emanating from an effusion source. Photocathodes were characterized as a function of antimony layer thickness and alkali consumption, inside a vacuum chamber that was initially baked, but frequently vented without re-baking. Photocathode lifetime measured at low voltage is correlated with the antimony layer thickness. Photocathodes manufactured with comparatively thick antimony layers exhibited the best lifetime. We speculate that the antimony layer serves as a reservoir, or sponge, for the alkali. © 2015 Author(s). All article content, except where otherwise noted, is licensed under a Creative Commons Attribution 3.0 Unported License. [<http://dx.doi.org/10.1063/1.4922319>]

Increasingly, new experiments and accelerator proposals dictate that photoguns provide very high current at high repetition rates. GaAs:Cs photocathodes can exhibit initial quantum efficiency (QE) of 10% or more at ~520 nm^{1,2} and can produce beams with small thermal emittance but they are fragile and require exceptionally good vacuum ($<2 \times 10^{-9}$ Pa)³ to avoid QE decay that results from ion back bombardment.⁴ For unpolarized beam applications, alkali-antimonide photocathodes represent a good alternative to delicate GaAs:Cs, providing similarly high QE but exhibiting less sensitivity to ion back bombardment. In the 1990s, Dowell *et al.* successfully fabricated CsK₂Sb photocathodes having 12% QE at 527 nm and generating then-record-level current from an RF gun.⁵ In addition, alkali-antimonide photocathodes with positive electron affinity are considered “prompt emitters” providing short electron bunches and small longitudinal emittance. Alkali-antimonide photocathodes describe a wide variety of compounds, including (Cs)Na₃KSb which has been shown to provide even higher QE than CsK₂Sb.¹ Interest in these photocathodes has been renewed as a result of new light source initiatives and proposed experiments that rely on high average current energy recovery linacs like the DarkLight experiment⁶ and a necessity to employ electron cooling of proton beams for recent electron ion collider proposals.⁷

Alkali-antimonide compounds are commonly used as photocathodes in photomultiplier tubes (PMTs)⁸ and in a few photoguns.^{5,9,10} Most PMTs operate in “transmission mode,” where incident light passes through a substrate before reaching the photocathode material, which must be very thin (~10–20 nm) to effectively transmit light to the emitting surface of the photocathode inside the phototube. In contrast, photoguns typically employ front face illumination of the photocathode (not transmission mode), in which case, the thickness of the photocathode is not a limiting factor, at least not in terms of how the light is delivered. Interestingly, most modern reports of bialkali-antimonide fabrication for photogun applications describe growing thin photocathodes similar to those used in PMTs and employing a recipe that relies on sequential deposition of K and Cs on a 15 nm thick Sb layer.¹¹ In this research, CsK₂Sb photocathodes were fabricated by co-deposition of both alkali

^aAuthor to whom correspondence should be addressed. Electronic mail: mmamu001@odu.edu



species using an *effusion source*^{12,13} on Sb layers with varying thickness (<50 nm–6.7 μm). The so-called effusion source was a common device used on dc high voltage photoguns from the 1970's through the 1990's, to fabricate GaAs:CsO photocathodes that possess a negative electron affinity. The effusion source was eventually replaced by the now widely used Cs₂CrO₄ based alkali source¹⁴ for GaAs photocathode applications, in large part because they are easier to use. However, for alkali-antimonide photocathode fabrication, the effusion source offers advantages over other alkali sources due to its relative high capacity and compact design with a small valve to isolate the alkali supply from the rest of the vacuum system. This allows alkali replacement without venting the rest of the deposition chamber.

Bialkali-antimonide photocathodes were grown by thermal evaporation of sources to achieve molecular beam epitaxy¹⁵ inside an ultrahigh vacuum chamber. Photocathodes were evaluated *in situ* at a low bias voltage of –284 V. The complete apparatus will be described in more detail in a subsequent publication. A brief description is given here. A polished p-doped bulk GaAs wafer was a convenient substrate choice because it required no special surface preparation steps to remove a native oxide layer, as is the case when using silicon. The GaAs substrate was attached to a long tube-shaped holder that could accommodate a heater. An annular tantalum cup of 2.54 cm outer diameter was used to secure the GaAs substrate to the sample holder and also served as a second substrate for the photocathode deposition. During deposition, the source to substrate distance was maintained at ~5 cm. The high-purity (99.9999%) Sb pellets from Alfa Aesar¹⁶ were resistively heated in a tungsten evaporation basket. The K (99.95% purity) and Cs (99.9 + % purity) sources consisted of 1 g breakseal ampoules from ESPI metals and Strem Chemicals, Inc., respectively, under 1 atm of argon gas pressure. Ampoules were inserted into the open end of a copper tube (1.27 cm dia.) with a mini-Conflat flange on one side that was attached to the control valve of the effusion source.¹² After pinching-off the open end of the copper tube, to make a vacuum tight seal, the copper tube was evacuated through the valve and heated to desorb water. The glass ampoules were then broken by slightly pinching the outside of the copper tube, cracking the glass ampoules and thus liberating the argon gas which was pumped away. To evaporate alkali metal during photocathode fabrication, hot air was passed through the heating tube that represents a central design feature of the effusion source, with the control valve open. The alkali temperature was kept constant by electrical feedback applied to the hot air source. To halt the flow of alkali, one simply closed the control valve.

Vacuum was maintained using non-evaporable getters (two GPI100 MK5 flange-mounted pumps and two WP950 NEG modules from SAES[®] Getters, with hydrogen pumping speed of 480 l s⁻¹ and 2300 l s⁻¹, respectively) and an ion pump (45 S Titan ion[™] pump from Gamma vacuum, nitrogen pumping speed of ~40 l s⁻¹). A turbo-molecular pump was used to pump down the apparatus, to achieve a vacuum level suitable to energize the ion pump. The vacuum was continuously monitored using the ion pump current. The chamber was initially baked at 200 °C for 180 h and then leak checked with helium using a residual gas analyzer (RGA) which also served as a chemical deposition rate monitor. Post bake, the chamber reached a vacuum of ~3 × 10⁻⁸ Pa. The chamber was repeatedly vented for loading new substrates without further baking of the system. Precautions were taken to minimize the amount of water vapor introduced to the system, namely, the apparatus was vented using nitrogen boil-off from a large LN₂ dewar; however, there was inevitable re-introduction of water vapor back into the apparatus. To the best of our knowledge, this is the first report of successful bialkali-photocathode fabrication inside a chamber that was baked once at the outset, but repeatedly vented and not re-baked. During the bialkali deposition, the chamber pressure typically reached >1 × 10⁻⁵ Pa and quickly improved to ~10⁻⁶–10⁻⁷ Pa once the deposition ended. The photocathodes were evaluated at vacuum pressures near 1 × 10⁻⁷ Pa inside the chamber with the RGA indicating the presence of water at partial pressure <2 × 10⁻⁸ Pa.

Before making photocathodes using all three chemicals, a field emission scanning electron microscope (FESEM) was used to assess Sb deposition characteristics for both substrates, as a function of deposition duration and as a function of applied current to the tungsten evaporation basket, with this information correlated to the partial pressure of Sb as registered by the RGA. The FESEM provided information on morphology, porosity, grain structure, and surface roughness as a function of Sb thickness, all of which represent important metrics that could help improve

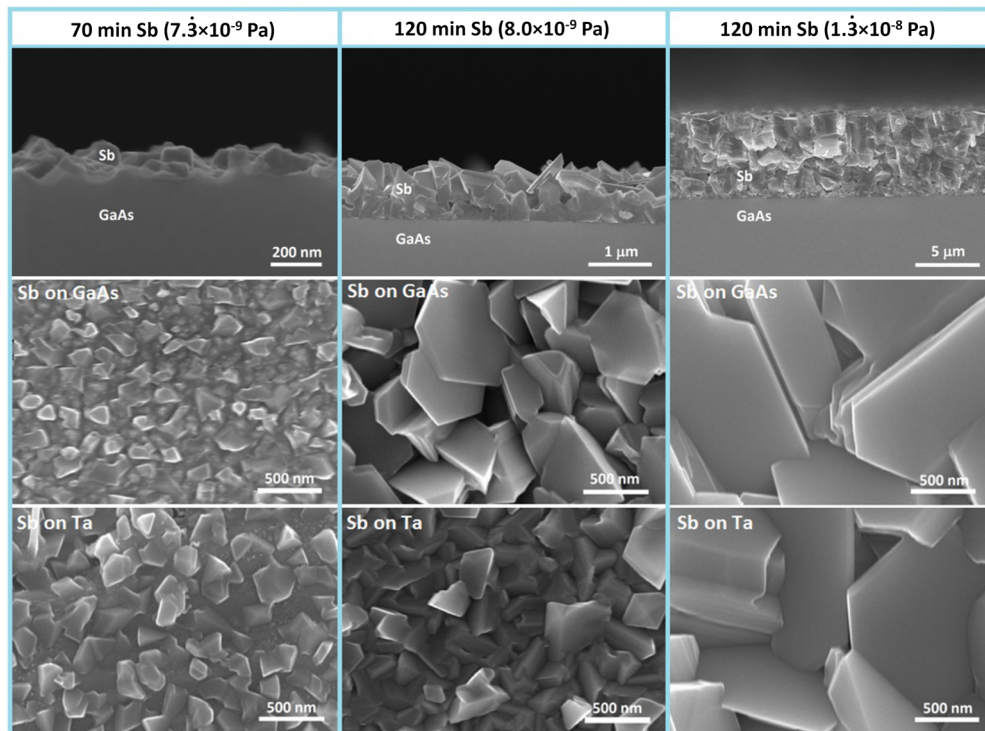


FIG. 1. FESEM images showing cross section and topographic views of Sb layers grown on GaAs (top and middle) and Ta (bottom) substrates, from left to right, conditions describing the growth of thicker Sb layers.

our understanding of the role of Sb layer on photocathode performance.^{5,10,17} These calibration measurements were conducted using a series of Sb films deposited on GaAs and Ta substrates under different conditions. The duration of deposition, and the rate of deposition, had a significant impact on the Sb layer thickness and morphology as illustrated in Figure 1. The Sb film thickness was defined as the distance from the substrate to the outermost edge of the antimony grains that formed. The Sb film thickness and Sb grain size varied dramatically over the evaluated parameter space, ranging from <50 nm to 6.7 μm and <20 nm to 2.5 μm , respectively. The porosity of the Sb film increased significantly with increasing Sb film thickness. In general, thin Sb films were more dense and smooth, compared to thick Sb films, which were more rough and porous.

Many photocathodes were made, but this work details the performance of five photocathodes, which were distinct with respect to the Sb layer thickness and morphology. Immediately prior to deposition, the substrates were heated to 550 $^{\circ}\text{C}$ for 2 h followed by rapid cooling to 200 $^{\circ}\text{C}$. Photocathodes were fabricated using a two-step deposition scheme: Sb was deposited first with substrate temperature maintained at 200 $^{\circ}\text{C}$, followed by a co-deposition of alkali species with substrate at 120 $^{\circ}\text{C}$. The Sb deposition time varied from 30 to 120 min and the deposition rate was varied by applying currents ranging from 31.2 to 33.7 A to the Sb heater basket. Under these deposition conditions, the partial pressure of the Sb vapor indicated by RGA was in the range of $7.3(\pm 0.6) \times 10^{-9}$ to $1.3(\pm 0.3) \times 10^{-8}$ Pa. Evaporation of combined alkali species was controlled by adjusting the heater power and the air flow rate applied to the effusion source and by regulating the control valve. The different parts of the effusion source were maintained at stable temperatures during alkali evaporation. To adjust the alkali deposition rate for different photocathodes, these temperatures were varied over the following ranges: the hot air inlet tube (381 - 462 $^{\circ}\text{C}$), the dispensing tube (232 - 294 $^{\circ}\text{C}$), and the reservoir tube (153 - 281 $^{\circ}\text{C}$). The QE was continuously monitored during the alkali deposition which continued until the QE was maximized and reached a plateau. Light from a low power (~ 4 mW) temperature-stabilized green laser (532 nm) was directed through a ring anode ~ 2.5 from the photocathode sample, illuminating the photocathode at normal incidence. The laser power was never attenuated, and no attempt was made to limit the extracted photocurrent which

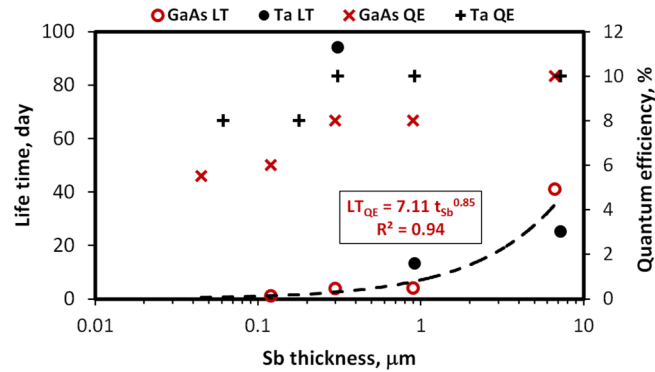


FIG. 2. QE and 1/e lifetime as a function of Sb thickness for CsK₂Sb photocathodes deposited on Ta and GaAs substrates. The photocathodes were biased at -284 V and illuminated with 4 mW of laser light at 532 nm.

for the best photocathodes could reach 200 μ A. Anode current unrelated to photoemission from the photocathode was less than 0.1% of the total measured current.

After fabrication, the photocathode was cooled to room temperature and QE was allowed to stabilize for 6–12 h. Then, QE of each photocathode was mapped across the entire substrate using the low power green laser. These QE measurements were repeated at different time intervals to evaluate photocathode QE lifetime, a metric describing the length of time required to observe QE decay to 1/e ($\sim 36.8\%$) of its initial value. When photocathodes are biased at high voltage and delivering beam to accelerators, different mechanisms play competing roles in QE decay, namely, ion bombardment and chemical poisoning of the activated photocathode surface.⁴ Inside a low voltage vacuum chamber like the one described in this paper, chemical poisoning is likely the dominant mechanism affecting lifetime. The maximum photocathode QE from both substrates and their corresponding 1/e lifetime are illustrated as a function of Sb thickness in Figure 2, where Sb thickness values represent estimates based on the FESEM calibration results described above. In general, there appears to be a weak QE dependence on the quantity of Sb applied to the substrate. Photocathodes with thin and thick layers of Sb provide comparable QE, assuming an appropriate amount of alkali was applied to maximize QE. The optimized photocathode QE for a tantalum substrate increased from $\sim 8\%$ to 10% over the range from thinnest (<50 nm) to thickest (6.7 μ m) Sb layers. For the GaAs substrate, QE increased from $\sim 6\%$ to 10% over the same range of Sb film thickness. In contrast, for photocathodes grown on the GaAs substrate, the low voltage QE lifetime exhibited a power-law dependence on Sb film thickness, with the longest lifetime (~ 42 days) obtained using the thickest Sb film (6.7 μ m). The lifetime results for photocathodes grown on the Ta substrate are harder to comprehend. The photocathode manufactured using a 300 nm Sb film provided photocurrent at 200 μ A for over 5 days, and a photocurrent decay experienced after a brief interruption resulted a 1/e lifetime in excess of 90 days. However, for thicker Sb layers, the observed lifetime of photocathodes grown on a Ta substrate followed a similar trend as those grown on the GaAs substrate. It must be pointed out however that extrapolating the performance based on measurements made relatively soon after photocathode fabrication, and over a comparatively short time period, is subject to error. And we are aware that lifetime measurements made at low voltage are not necessarily directly applicable to beam-based lifetime measurements made at high voltage. Nevertheless, the spontaneous evaluation of microstructures and QE at low voltage is important for managing the quality of photocathodes.

The low power laser was replaced with a wavelength tunable light source¹⁸ to measure QE as a function of wavelength from 425 to 825 nm (Figure 3), for the photocathode fabricated using a rough porous 300 nm Sb layer (inset), on Ta and GaAs substrates. Both substrates exhibited similar distribution of QE $> 21\%$ at 425 nm. This spectral response correlates well with the reference curve representative of typical bialkali-antimonide photocathodes used in PMTs,¹⁹ which likely indicates good stoichiometry of our photocathodes grown by co-deposition of alkalis.²⁰ The co-deposition thus enabled optimal stoichiometry of photocathodes with very thick Sb layers compared to the traditional photocathode recipe where K and Cs are sequentially deposited on a 15 nm Sb layer.¹¹

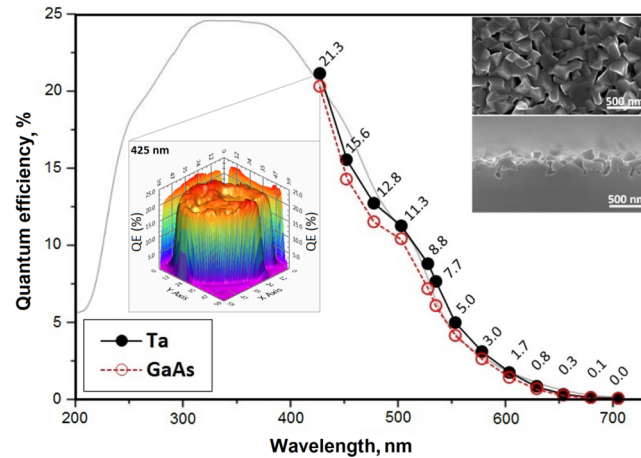


FIG. 3. The spectral response of CsK₂Sb photocathode deposited on Ta and GaAs substrates. QE distribution at 425 nm is shown in inset. The photocathode was prepared by bialkali co-deposition on a 300 nm Sb layer.

To glean insight related to photocathode stoichiometry, the relative amount of source materials required for each QE-optimized photocathode was estimated by noting the duration of deposition, and the partial pressure of each chemical species as indicated by the RGA, and using the following formula:

$$Q = \frac{t \cdot P}{t_o \cdot P_o}, \quad (1)$$

where Q represents the normalized quantity of a particular chemical species, relative to the Cs amount applied to the photocathode manufactured with the thinnest Sb layer, denoted by the index o . The quantities t represent the time duration of deposition, and P the RGA detected partial pressure of each species. Figure 4 illustrates that for a QE-optimized photocathode, the required amount of Cs and K depends strongly on the amount (or thickness) of Sb applied to the substrate. The Sb thickness increases exponentially with the applied amount of Sb. Notice that the required quantity of Cs and K increased in a similar manner and exhibited a power-law dependence on the Sb film thickness.

To explain some of the observations reported here, we speculate that photocathode performance using relatively thick Sb layers depends heavily on the surface morphology of the Sb film. In general, thin Sb films are smooth and dense compared to thicker Sb films which exhibit a high degree of roughness and porosity. The Sb likely initially forms discontinuous nucleation on the substrates.

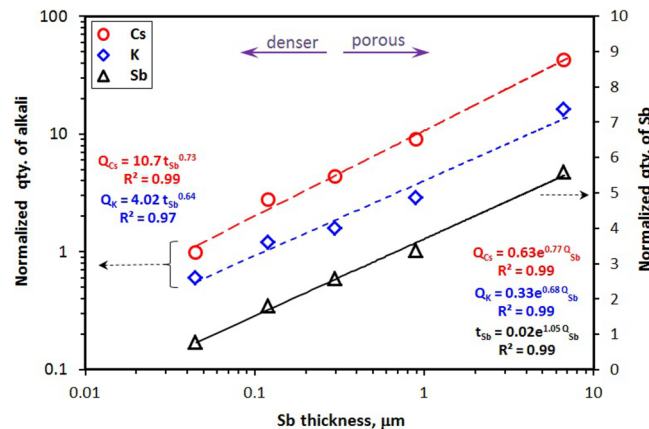


FIG. 4. Normalized quantity of source materials for optimal QE as a function of Sb thickness for CsK₂Sb photocathodes manufactured via co-deposition of alkali species.

With further addition of Sb, the nucleation saturation occurs and a full surface coverage by Sb grains is obtained. With continued addition of Sb, the film subsequently grows increasingly thicker and exhibits larger grain structure with increased inter-granular voids (see Figure 1), which serves to increase the envelope surface area of Sb grains. The required amount of alkalis for optimum QE will depend on the effective surface area to volume ratio. It is clear that thicker layers of Sb serve to “store” more alkalis. The QE lifetime results shown in Figure 2 indicate that photocathodes with more alkali storage provide longer lifetime in a manner similar to that of porous substrates used in a dispenser photocathodes²¹ which serve as an alkali-reservoir.

In summary, the Sb-layer morphology has been studied and the optical performance of photocathodes has been correlated with the Sb thickness and alkali consumption, where thick Sb layers exhibited the best lifetime at low voltage. The photocathodes were grown on GaAs and Ta substrates in a chamber which was not baked following venting and loading of new substrates. A field emission scanning electron microscope was used to evaluate the Sb-layer morphology as a function of Sb-layer thickness and to correlate the latter with partial pressures registered by the RGA, therefore allowing us to use it as a chemical deposition rate monitor. Thin Sb layers provide a relatively dense smooth surface, whereas thick Sb layers appear porous with increased surface roughness. The high-capacity effusion source enabled us to successfully manufacture bialkali-antimonide photocathodes having maximum QE around 10% and extended lifetime (>90 days) at 532 nm via the co-deposition method, with relatively thick layers of antimony (≥ 300 nm). The effusion source offers advantages over other alkali sources. We believe co-deposition supports the formation of bialkali-antimonide photocathodes with thick antimony layer compared to those manufactured using sequential deposition. We speculate that the antimony layer serves as a reservoir, or sponge, for the alkalis in the CsK₂Sb photocathodes. Photocathodes such as these will be tested inside a dc high voltage photogun in the coming months, where we expect to correlate some of the observations reported here, with measurements of beam quality including beam emittance.

This material is based on work supported by the U.S. Department of Energy, Division of Material Sciences, under Grant No. DE-FG02-97ER45625 and the National Science Foundation Grant No. DMR-0420304. We also acknowledge college of William and Mary, and Dr. Kai Zhang of ODU for using the FESEM for the microscopic imaging.

- ¹ D. Dowell, I. Bazarov, B. Dunham, K. Harkay, C. Hernandez-Garcia, R. Legg, H. Padmore, T. Rao, J. Smedley, and W. Wan, *Nucl. Instrum. Methods Phys. Res., Sect. A* **622**, 685 (2010).
- ² *Cornell Energy Recovery Linac: Science Case Project Definition Design Report*, edited by G. H. Hoffstaetter, S. M. Gruner, and M. Tigner (2013), see <http://www.classe.cornell.edu/rsrc/Home/Research/ERL/PDDR/PDDR.pdf>.
- ³ N. Chanlek, J. D. Herbert, R. M. Jones, L. B. Jones, K. J. Middleman, and B. L. Militsyn, *J. Phys. D: Appl. Phys.* **47**, 055110 (2014).
- ⁴ C. K. Sinclair, P. A. Adderley, B. M. Dunham, J. C. Hansknecht, P. Hartmann, M. Poelker, J. S. Price, P. M. Rutt, W. J. Schneider, and M. Steigerwald, *Phys. Rev. Spec. Top.—Accel. Beams* **10**, 023501 (2007).
- ⁵ D. H. Dowell, S. Z. Bethel, and K. D. Friddell, *Nucl. Instrum. Methods Phys. Res., Sect. A* **356**, 167 (1995).
- ⁶ J. Balewski, J. Bernauer, W. Bertozzi, J. Bessuille, B. Buck, R. Cowan, K. Dow, C. Epstein, P. Fisher, S. Gilad, E. Ihloff, Y. Kahn, A. Kelleher, J. Kelsey, R. Milner, C. Moran, L. Ou, R. Russell, B. Schmookler, J. Thaler, C. Tschalär, C. Vidal, A. Winnebeck, S. Benson, C. Gould, G. Biallas, J. R. Boyce, J. Coleman, D. Douglas, R. Ent, P. Evtushenko, H. C. Fenker, J. Gubeli, F. Hannon, J. Huang, K. Jordan, R. Legg, M. Marchlik, W. Moore, G. Neil, M. Shinn, C. Tennant, R. Walker, G. Williams, S. Zhang, M. Freytsis, R. Fiorito, P. O’Shea, G. Ovanesyan, T. Gunter, N. Kalantarians, M. Kohl, I. Albayrak, M. Carmignotto, T. Horn, D. S. Gunarathne, C. J. Marto, D. L. Olivitt, B. Surrow, X. Lia, R. Beck, R. Schmitz, D. Walther, K. Brinkmann, and H. Zaunig, “DarkLight: A search for dark forces at the Jefferson laboratory free-electron laser facility,” e-print [arXiv:1307.4432v2](https://arxiv.org/abs/1307.4432v2) [physics.ins-det] (2013).
- ⁷ A. W. Thomas, “An electron-ion collider at Jefferson lab,” e-print [arXiv:0907.4785v1](https://arxiv.org/abs/0907.4785v1) [hep-ex] (2009).
- ⁸ D. E. Persyk, J. Morales, R. McKeighen, and G. Muehllehner, “The quadrant photomultiplier,” *IEEE Trans. Nucl. Sci.* **26**, 364–367 (1979).
- ⁹ F. Sannibale, B. Bailey, K. Baptiste, A. Catalano, D. Colomb, J. Corlett, S. De Santis, L. Doolittle, J. Feng, D. Filippetto, G. Huang, R. Kraft, D. Li, M. Messerly, H. Padmore, C. F. Papadopoulos, G. Portmann, M. Prantil, S. Prestemon, J. Qiang, J. Staples, M. Stuart, T. Vecchione, R. Wells, M. Yoon, and M. Zolotarev, “Status of the LBNL normal-conducting CW VHF electron photo-gun,” in *Proceedings of the 2010 Free Electron Laser Conference, Malmo, Sweden, August* (2010).
- ¹⁰ L. Cultrera, I. Bazarov, J. Conway, B. Dunham, Y. Hwang, Y. Li, X. Liu, T. Moore, R. Merluzzi, K. Smolenski, S. Karkare, J. Maxson, and W. Schaff, “Photocathode R&D at Cornell University,” in *Proceedings of IPAC2012, New Orleans, Louisiana, USA* (JACoW, 2012), WEOAB02, p. 2137.
- ¹¹ J. Smedley, K. Attenkofer, S. G. Schubert, H. A. Padmore, J. Wong, J. Xie, M. Ruiz-Oses, I. Ben-Zvi, X. Liang, E. M. Muller, and J. DeFazio, “Alkali antimonide photocathodes for everyone,” in *Proceedings of IPAC2013, Pasadena, California, USA* (JACoW, 2013), THPAC17, pp. 1178.

- ¹² D. M. Dunham and C. K. Sinclair, "Charging the cesiator on the Illinois/CEBAF polarized electron source," in *NPL Polarized source Group Technical Note # 90-9, Nuclear Physics Laboratory* (University of Illinois at Urbana-Champaign, IL, USA, 1990).
- ¹³ C. Y. Prescott, W. B. Atwood, R. L. A. Cottrell, H. Destaebler, E. L. Garwin, A. Gonidec, R. H. Miller, L. S. Rochester, T. Sato, D. J. Sherden, C. K. Sinclair, S. Stein, and R. E. Taylor, *Phys. Lett. B* **77**, 347 (1978).
- ¹⁴ M. Succi, R. Canino, and B. Ferrario, *Vacuum* **35**, 579 (1985).
- ¹⁵ V. V. Balanyuk, A. S. Chernikov, V. F. Krasnov, S. L. Musher, V. E. Ryabchenko, A. M. Prokhorov, I. A. Dubovoi, V. K. Ushakov, and M. Y. Schelev, *SPIE Adv. Process. Semicond. Devices* **945**, 68 (1988).
- ¹⁶ Alkali Metal Dispensers Brochure 1789, SAES getters, 20020 Lainate (MI) Italy (2007).
- ¹⁷ T. Vecchione, I. Ben-Zvi, D. H. Dowell, J. Feng, T. Rao, J. Smedley, W. Wan, and H. A. Padmore, *Appl. Phys. Lett.* **99**, 034103 (2011).
- ¹⁸ NKT Photonics A/S Blokken 84, DK-3460 Birkerød Denmark see <http://www.nktphotonics.com/superkextreme>.
- ¹⁹ M. Suyama, "Latest status of PMTs and related sensors," in *Proceedings of the International Workshop on New photon-detectors, PoS (PD07) 018, Kobe, Japan, June 27-29 (2007)*.
- ²⁰ P. Michelato, *Nucl. Instrum. Methods Phys. Res Sect. A* **393**, 455 (1997).
- ²¹ E. J. Montgomery, D. W. Feldman, P. G. O'Shea, Z. Pan, N. Sennett, K. L. Jensen, and N. A. Moody, *J. Directed Energy* **3**, 66 (2008).